Available online at www.sciencedirect.com
SCIENCE DIRECT
Journal of Molecular Catalysis A: Chemical 244 (2006) 73–82
JOURNAL OF MOLECULAR CATALYSIS A: CHEMICAL
www.elsevier.com/locate/molcata

Effect of calcination temperature on the photocatalytic activity and adhesion of TiO_2 films prepared by the P-25 powder-modified sol–gel method

Yongjun Chen, Dionysios D. Dionysiou *

Department of Civil and Environmental Engineering, University of Cincinnati, Cincinnati, OH 45221-0071, USA

Received 11 June 2005; received in revised form 26 August 2005; accepted 26 August 2005
Available online 7 October 2005

Abstract

TiO_2 films on 304 stainless steel with optimum P-25 loading (PPMSGFs-50) were prepared by the P-25 powder-modified sol–gel method (PPMSGM) at calcination temperatures from 400 to 700 °C. The as-prepared PPMSGFs-50 were characterized by differential scanning colorimetry/thermogravimetric analyses (DSC/TGA), scanning electron microscopy (SEM), TEM/high-resolution transmission electron microscope (HR-TEM), X-ray diffraction (XRD), N_2 adsorption and X-ray photoelectron spectroscopy (XPS). Their adhesion properties were tested by the scratch test and cross-hatch adhesion test and their photocatalytic activities were evaluated using 4-CBA as a model organic contaminant in water. It was found that decreasing calcination temperature leads to a decrease in the critical loading, which has a detrimental effect on the mechanical stability of the films. On the other hand, decreasing calcination temperature leads to an enhancement of photocatalytic activity. The optimum calcination temperature is 500 °C under which both enhanced photocatalytic activity and good adherence on the support could be obtained. The 4-CBA removal efficiency for PPMSGF-50 at 500 °C was approximately four times that of PPMSGF-50 at 600 °C after 10 h of photocatalytic oxidation. Increasing calcination temperature in the range between 500 and 700 °C caused a significantly increase in the diffusion of foreign metals (i.e. chromium, iron and manganese) from the stainless steel support to the TiO_2 film. It is believed that the enhancement of the photocatalytic activity at lower calcination temperatures (400–500 °C) is due to an increase in the amount of two type of crystallites exposed to the solid–liquid interface and decrease in foreign metal ion concentrations (i.e. Cr^{3+}) on the surface of the films.

Keywords: Photocatalysis; Active sites; Adhesion; Degussa P-25; Immobilized

1. Introduction

Since the pioneering discovery of the photocatalytic properties of TiO_2 [1] and the demonstration of its effectiveness to generate hydroxyl radicals when illuminated with UV light along with its environmentally benign properties (i.e. non-toxicity, absence of dissolution in water and photostability), and relatively low cost, TiO_2 photocatalyst has been considered a key material in the destruction of recalcitrant organic pollutants in water [2–10]. While most initial studies in the area of TiO_2 photocatalysis have utilized TiO_2 nanoparticles in suspension, the use of TiO_2 catalyst immobilized on appropriate supports is becoming more popular because this approach eliminates the need to filter the TiO_2 nanoparticles in suspension, which is an expensive and tedious process.

Recently, a new family of TiO_2 "thick" films developed by Balasubramanian et al. using a P-25 powder-modified sol–gel method (PPMSGM) exhibited enhanced photocatalytic activity and hardness compared to those obtained using a conventional ("unmodified") sol–gel procedure [11,12]. Because of their potential to satisfy several important requirements (high photocatalytic activity, good adhesion to the support and resistance to attrition), such films are of great interest for the development of high performance photocatalytic reactors for water treatment and reuse in both terrestrial and space applications [13].

The calcination temperature is an important parameter in the synthesis of ceramic materials and catalysts using sol–gel methods and can play a critical role in controlling the physicochemical properties of such immobilized films. In fact, it has been previously reported that the photocatalytic activity of TiO_2 films is greatly affected by the calcination temperature [14,15]. In addition, the mechanical stability of such films is also dependent on calcination temperature [16,17]. Therefore, in order to develop high performance photocatalytic films prepared by

* Corresponding author. Tel.: +1 513 556 0724; fax: +1 513 556 2599.
E-mail address: dionysios.d.dionysiou@uc.edu (D.D. Dionysiou).

1381-1169/$ – see front matter © 2005 Elsevier B.V. All rights reserved.
doi:10.1016/j.molcata.2005.08.056

sol–gel methods and modifications, it is important to understand the relationship between calcination temperature and photocatalytic activity and mechanical stability of such films. Continuing the initial work of Balasubramanian et al. [11,12], we have recently optimized the PPMSGM with respect to the loading of P-25 powder added in the alkoxide sol and the photocatalytic activity of such films [18]. It was found that 50 g/L of P-25 was the optimum and that under such conditions the films (PPMSGF-50) prepared by this method exhibited enhanced photocatalytic activity and good mechanical stability.

However, the effect of calcination temperature on the photocatalytic activity and adhesion of PPMSGF-50 catalyst has not yet been reported. Therefore, the objective of this study is to determine whether the photocatalytic activity of PPMSGF-50 can be further improved while maintaining good adhesion to the support, only by changing the calcination temperature. In this study, PPMSGF-50 films prepared under different calcination temperatures were evaluated for their adsorption capacity for a model organic contaminant and were characterized using DSC/TGA, XRD, HR-TEM/TEM, SEM, N_2 adsorption and XPS to obtain insights on the relationship of absorbability, crystal structure, morphology, specific surface area (BET), pore volume and surface chemical composition to the photocatalytic activity. Finally, the strength of adhesion of PPMSGF-50 films was tested by the scratch and cross-hatch tape tests.

2. Experimental

2.1. Synthesis of PPMSGF-50

A flowchart for the preparation of PPMSGF-50 is shown in Fig. 1. This procedure is similar to that published previously by Balasubramanian et al. [11,12]. Commercial ultra pure titanium isopropoxide (TTIP, Aldrich), isopropanol (*i*-PrOH, Fisher Scientific), diethanolamine (DEA, Fisher Scientific) and nanophase TiO_2 Degussa P-25 powder (50 m^2/g; 15–30% rutile + 85–70% anatase, mean diameter of 30 nm) were used for the preparation of the modified sol. A 0.5 M solution of TTIP in *i*-PrOH was prepared and a calculated amount of DEA was added to the solution. A molar ratio of DEA/TTIP of 4 was used. The solution was stirred at room temperature for approximately 2 h. Subsequently, water was added drop-wise under vigorous stirring conditions. A molar ratio of H_2O/TTIP of 2 was used. A clear and stable alkoxide sol was obtained using this process. The titania modified sol was prepared by adding 50 g/L Degussa P-25 TiO_2 powder into the alkoxide sol. The powder was added slowly under vigorous stirring to prevent the formation of agglomerates. A thick, white, viscous suspension was obtained. This modified sol was being stirred rapidly to prevent precipitation in storage between experiments.

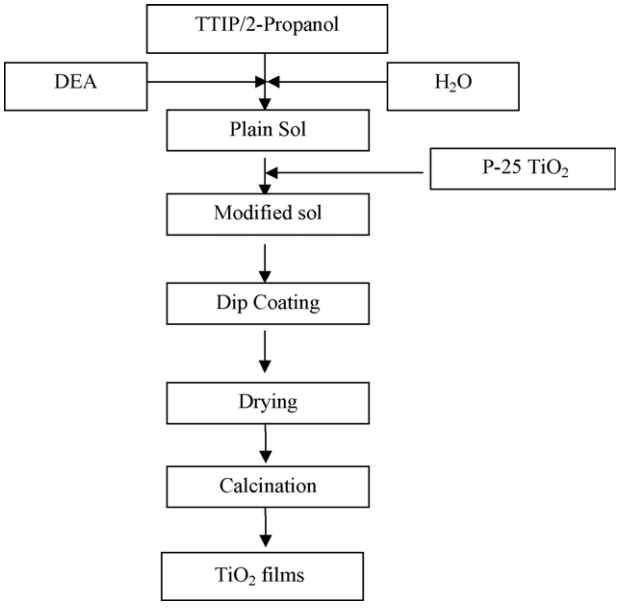

Fig. 1. Schematic of the preparation steps in the TiO_2 powder-modified sol–gel method.

The uncoated 304 stainless steel substrates were cleaned with ethanol and methyl ethyl ketone (99.8%, Fisher Scientific). The clean substrates were dried at 125 °C for 24 h. A dip coating apparatus equipped with a velocity-control adjustable motor was used to dip in and pull out the substrate at a preset constant velocity. A withdrawal velocity of 12.3 ± 0.5 cm/min was used in this study. After the dip coating procedure was completed, the coatings were dried at room temperature for 24 h, and then placed into a multi-segment programmable high temperature furnace (Paragon Model HT-22-D, Thermcraft Inc., Winston-Salem, NC) for calcination. The furnace temperature was incremented at a ramp rate of 3.0 °C/min until 100 °C was reached and this temperature was held for 1 h. The temperature of the oven was increased at a rate of 3.0 °C/min to a final temperature (400–700 °C) and again held for 1 h. Finally, the coatings were cooled naturally to room temperature (approximately a 15 h cooling period).

2.2. Characterization of PPMSGF-50 films

The crystal phase composition of PPMSGF-50 films was determined by X-ray diffraction (XRD) using a Siemens Kristalloflex D500 diffractometer with Cu Kα radiation. The surface microstructure was characterized by scanning electron microscopy (SEM; Hitachi S-4000) and the surface composition of PPMSGF-50 films was determined by X-ray photoelectron spectroscopy (XPS). An Mg Kα X-ray source was used with pass energy of 35.75 eV for the high-resolution spectra. The adhesion between PPMSGF-50 films and the stainless steel substrate was examined using a Sebastian V scratch tester (Spokane, WA) and the cross-hatch adhesion test according to ASTM method D 3359B-02 [19]. Differential scanning colorimetry/thermogravimetric analyses were performed using a SDT 2960 DSC/TGA instrument with a heating program at 5 °C/min and gas flow rate at 100 mL/min in air atmosphere. The crystal size of the TiO_2 particles in the PPMSGF-50 films was determined by a JEM-2010F (JEOL) high-resolution transmission electron microscope (HR-TEM) with field emission gun at 200 kV. The samples were dispersed in methanol (HPLC grade, Pharmco) using an ultrasonic cleaner (2510R-DH, Bransonic) for 5 min and fixed on a carbon-coated copper grid (LC200-Cu,

EMS). Pore volume and specific surface area of the films were measured by Micromeritics TriStar 3000 Gas Absorption Analyzer.

2.3. Photocatalytic activity evaluation of PPMSGF-50 films

The photocatalytic activity of the PPMSGF-50 films was evaluated using 4-chlorobenzoic acid (99%, Aldrich, Milwaukee, WI) aqueous solution with an initial concentration of approximately 48 mg/L. The pH of the solution was adjusted to 3.0 using dilute HNO_3 solution, so as to keep the same pH of the solution during the reaction. The photocatalytic reactor used was a rectangular quartz unit with inside dimensions of 1 cm × 10 cm × 25 cm connected to a 500 mL container. The container was used for sampling and aeration of the solution. The dimensions of the coatings dipped into 4-CBA solution were 24 cm (length) × 8 cm (width). The UV source consisted of four 15 W integrally filtered low-pressure mercury UV tubes (Spectronics Corp., Westbury, NY) emitting radiation with wavelength in the range 300–400 nm and a peak at 365 nm. The average intensity of the UV radiation for each tube was approximately 1050 μW/cm^2 measured by a UV radiation meter (IL 1700 International Light, Serial No. 2547) at a distance of 12.5 cm from the center of the tube. The tubes were mounted in pairs in two silver-anodized housings positioned vertically on opposite sides of the quartz reactor at a distance of 12.5 cm. The solution in the container connected to the reactor was bubbled using humidified air with a flow rate of 2 L/min. The reactor was cooled by a fan (Duracraft Corporation, South Borough, Massachusetts) positioned near the reactor. During the reaction, the solution temperature increased gradually from 24 to around 26 °C within the first 2 h and was maintained at around 26 °C with the aid of the fan. The concentration of the 4-CBA in the samples was analyzed using HPLC (Agilent 1100 series) equipped with a diode array detector (DAD) and an autosampler. The stationery phase used was a C-16 column (Supelco Corporation). The mobile phase composition was H_2SO_4 (0.01N) 60% (v/v) and acetonitrile 40% (v/v).

3. Results and discussion

3.1. XRD and HR-TEM

Fig. 2 shows XRD spectra of PPMSGF-50 films prepared at different calcination temperatures from 400 to 700 °C. In the range of 400–600 °C, there is a sharp peak at 25.4° and a small peak at 27.5°, which correspond to anatase (1 0 1) and rutile (1 1 0), respectively. The peak intensity of anatase (1 0 1) is similar for PPMSGF-50 films prepared at calcination temperatures in the range between 400 and 600 °C, which demonstrates similar quantities of anatase (1 0 1) crystallites. When the calcination temperature reaches 700 °C, the peak intensity of anatase (1 0 1) remarkably decreases and the peak intensity of rutile (1 1 0) significantly increases, which demonstrates that most anatase (1 0 1) phase has been transformed into rutile (1 1 0) phase. At 700 °C, other crystal planes, such as anatase (1 0 3) and rutile (2 1 1) are also observed.

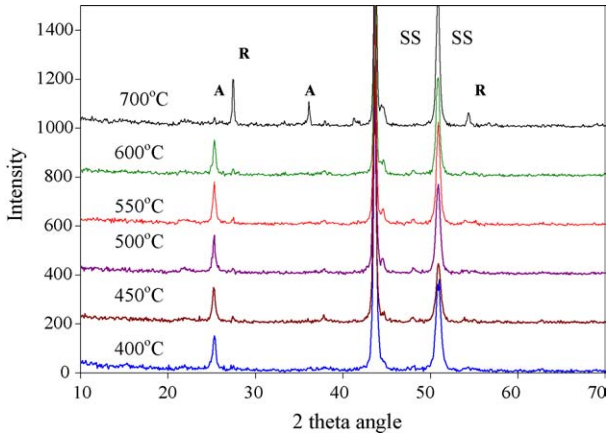

Fig. 2. X-ray diffraction spectra of PPMSGF-50 films prepared at different calcination temperatures (one dip coating layer).

Table 1 summarizes results of the crystal size calculated using the Scherrer's equation based on the half peak width and measured using TEM/HR-TEM. These results will be discussed in detail in the following part. Fig. 3 shows TEM/HR-TEM images of PPMSGF-50 films prepared at 400, 500, 600 and 700 °C calcination temperature. The TEM images clearly show that the average crystal size increases significantly as the calcination temperature increases from 500 to 700 °C and that the results agreed reasonably well with the results obtained based on the XRD analysis. On the other hand, the size and shape of the crystallites in each PPMSGF-50 film are also quite different. PPMSGF-50 films, like other P-25 powder-modified films [11,12], are composite films that contain crystallites from Degussa P-25 and those formed from the alkoxide hydrolysis [18]. It can be observed from Fig. 3(c and d) that the average crystal size of larger crystallites is approximately 30 nm. Considering that the average crystal size of Degussa P-25 is around 30 nm, the larger crystallites in the PPMSGF-50 films are most probably originated from Degussa P-25 crystallites. The crystallites with smaller size are most probably those formed from alkoxide hydrolysis and condensation in the sol. The above results suggest that the fine grains (aggregates with distinct boundaries) are composed of a mixture of the crystallites from Degussa P-25 and those formed from the alkoxide hydrolysis. According to the results summarized in Table 1, the crystal size ranges are

Table 1
Crystal size, fine grain size, BET and total pore volume of PPMSGF-50 films at different calcination temperatures

Temperature (°C)	400	500	600	700
Crystallite size from XRD[a]	28 ± 1	28 ± 1	31 ± 1	–
Crystallite size from TEM[b]	15–33	15–34	28–41	93–164
Average fine grain size (nm)[c]	96	48	60	143
BET (m^2/g)[d]	82.11	55.83	30.75	4.61
Total pore volume[e] (g/cm^3)	0.149	0.142	0.103	0.054

[a] Using Scherrer equation for anatase (1 0 1).
[b] HR-TEM.
[c] A cluster of crystallites on the surface of the film in Fig. 5.
[d] Samples are obtained after one heating cycle.
[e] Single point desorption total pore volume of pores at $P/P_o = 0.98$.

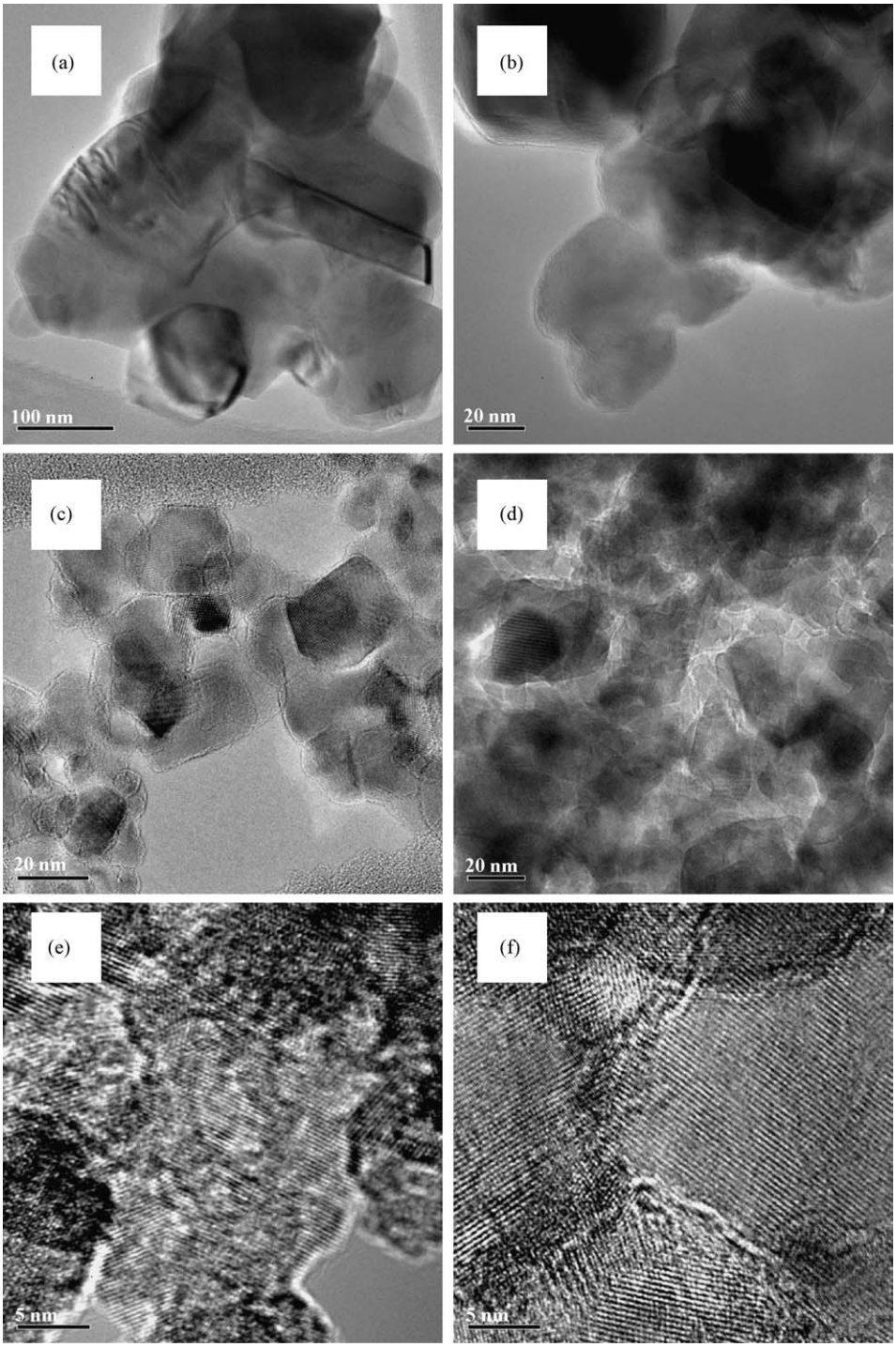

Fig. 3. HR-TEM of PPMSGF-50 films at different calcination temperatures (a) 700 °C, (b) 600 °C (different Degussa P-25 batch), (c and e) 500 °C and (d and f) 400 °C.

15–34, 28–41 and 93–164 nm for films calcined at 500, 600 and 700 °C, respectively. The crystal size range of films calcined at 400 and 500 °C are similar. Therefore, the size of crystallites originated from P-25 and formed from alkoxide hydrolysis increases when the calcination temperature is increased above 500 °C. In addition, as shown in Fig. 3(e and f), the crystallites of PPMSGF-50 present clear lattice fringes. It is possible that the amorphous gel formed from the alkoxide hydrolysis and condensation completely crystallized into anatase phase when calcination temperature reaches 400 °C.

3.2. TGA and DSC

In order to better understand the behavior of the hybrid gel prepared with 50 g/L P-25 loading in the sol during different heat treatment conditions, the as-prepared sample was analyzed

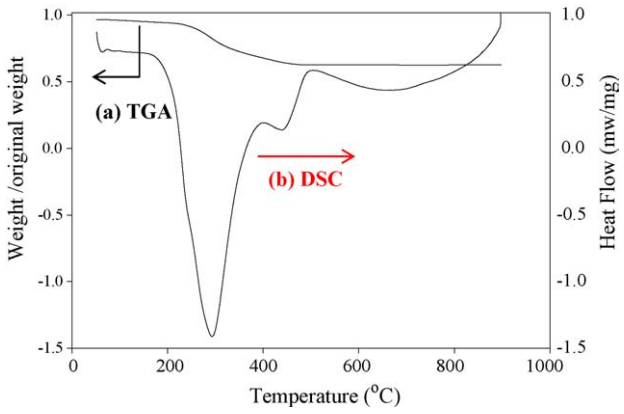

Fig. 4. (a) TGA and (b) DSC curve of hybrid gel dried at 100 °C.

using DSC/TGA at a rate of 5 °C/min in air. The sample was obtained by scratching the hybrid gel from the stainless steel substrate after drying at 100 °C for 1 h. As shown in Fig. 4(a), there are three stages in the TGA curve. In the range between 52 and 236 °C, the weight loss is 3.53%, which is attributed to the evaporation of adsorbed water and isopropanol. In the range between 236 and 464 °C, the weight loss is approximately 33.3% and it is attributed to the evaporation of DEA (the boiling point is 268.8 °C) and combustion of organic compounds including DEA, residual isopropanol and other organic intermediates after thermohydrolysis in the gel. Meanwhile, the decomposition of organic compounds also produces a sharp exothermic peak at 300 °C in the DSC curve (Fig. 4(b)). After 464 °C, no obvious weight change in the TGA curve can be observed, which demonstrates that most organic compounds have been eliminated at temperatures lower than 464 °C. According to Fig. 4(b), it is noticed that there is another small exothermic peak at 446 °C, which should correspond to the transformation of amorphous phase to anatase phase. This result seems not to correspond to the results of crystallite analysis obtained by XRD and HR-TEM. This is because the samples for HR-TEM and XRD analysis were taken after heat treatment of the as-prepared gel to the final temperature for 1 h, whereas the DSC analysis was performed under non-isothermal conditions [20]. Therefore, the actual phase transformation of the PPMSGFs-50 has started before 446 °C.

3.3. Film morphology and thickness

Fig. 5 shows SEM micrographs of PPMSGF-50 films at different calcination temperatures at a magnification of 40,000. It can be clearly seen that the surface of all PPMSGF-50 films are full of fine grains. In addition, the presence of intra-aggregate and inter-aggregate pores as well as microcracks on the surface of PPMSGF-50 can be clearly seen. The size of fine grains in the PPMSGF-50 films calcined at 400 °C is around 96 nm. However, it significantly decreases to 48 nm for films calcined at 500 °C, which is the smallest grain size among PPMSGF-50 films calcined at temperatures between 400 and 700 °C. From Figs. 2 and 3(f), it can be seen that the amorphous phase has been completely transformed to anatase phase at 400 °C calcination. Moreover, it is possible that no significant crystal sintering takes place at such a low calcination temperature. According to Fig. 4, it is observed that the organic residuals cannot be fully removed at 400 °C. Therefore, it can be concluded that crystallites formed from the alkoxide hydrolysis and in the presence of

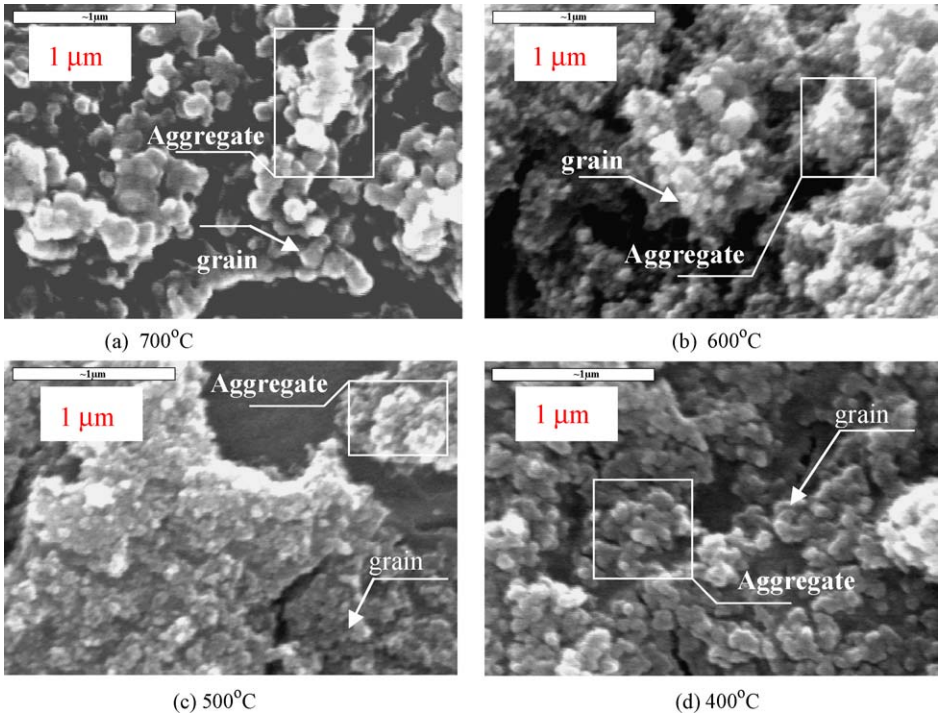

Fig. 5. Scanning electron micrographs of the surface of PPMSGF-50 films at different calcination temperatures.

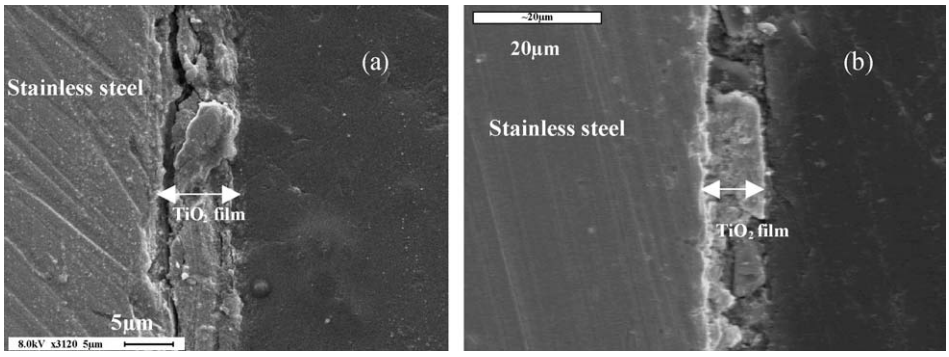

Fig. 6. Cross-section SEM for film thickness of PPMSGF-50 films at (a) 500 °C and (b) 400 °C.

some residual organic content aggregate loosely surrounding P-25 crystallites and for this reason the grain size looks larger. At 500 °C, the organic residuals can be effectively removed (as shown in Fig. 4) and the film is further consolidated. As a result, the larger grains "break" into smaller grains. When the calcination temperature reaches 600 °C, the size of some grains increases due to increased crystal size caused by sintering of some crystallites. At 700 °C, the grain size further increases reaching approximately 143 nm. This is because such large grain size is induced by the phase transformation of most anatase to rutile (as shown in Fig. 2).

Figs. 6 and 7 show results on the effect of calcination temperature on film thickness as measured by cross-section SEM. There is an obvious decrease in the film thickness from approximately 10 to 6.7 μm as the calcination temperature increases from 400 to 500 °C. The change in film thickness proves that film shrinkage took place as the calcination temperature increased from 400 to 500 °C. As a result, the crystalline material of the film is consolidated at 500 °C, which can be beneficial for enhancing attrition resistance. Moreover, there is no obvious difference in film thickness for films calcined at 500 and 600 °C, which demonstrates that no further shrinkage of the film takes place in this temperature range. However, when the calcination temperature increases to 700 °C, the film thickness reaches approximately 9.3 μm most probably due to increase in crystallite and grain sizes with an increase in calcination temperature from 600 to 700 °C. Previous literature has reported that larger grain size can produce thicker films [11].

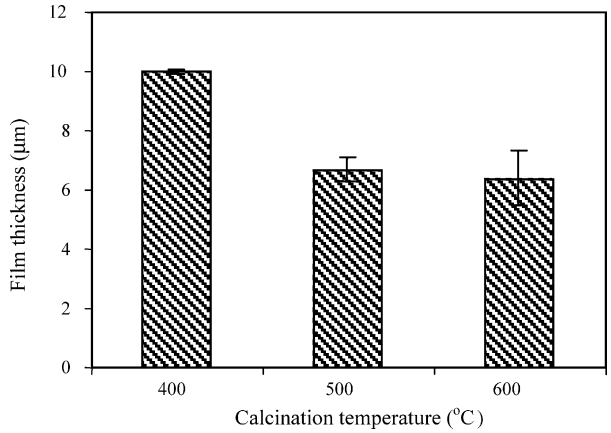

Fig. 7. Film thickness of PPMSGF-50 films at different calcination temperatures.

Table 2
Elemental composition of 304 stainless steel (EDS analysis)

Element	O	Si	Ti	Cr	Fe	Ni	Total
wt%	3.76	0.45	0.03[a]	18.63	69.03	8.10	100.00
at%	11.86	0.81	0.03[a]	18.05	62.30	6.95	100.00

[a] ≤2 sigma.

3.4. XPS analysis

Considering possible metal ion diffusion from the stainless steel support during calcination at high temperatures, we carried out a systematic study for the metal composition at the surface of PPMSGF-50 films as a function of calcination temperature. Table 2 presents the metal composition of 304 stainless steel obtained by EDS analysis. According to the results, Cr, Fe and Ni are the main components of 304 stainless steel. It should be noted that although EDS analysis did not detect Mn, the information provided by the manufacturer indicates also the presence of small amounts of Mn. Table 3 shows the relative percentage of metals on the surface of PPMSGF-50 films at different calcination temperatures. The results show that increasing calcination temperature results in an enhancement of the concentration of foreign metal including Cr, Fe and Mn on the surface of the coatings. This is due to the diffusion of these species from the stainless steel support to the surface of the films and that this rate of diffusion increases as the calcination temperature increases. It can also be noted that Cr is the main foreign metal element on the surface of the films. At the same time, high-resolution

Table 3
Metal composition of the surface of PPMSGF-50 films (two dip coating layers) at different calcination temperatures

Temperature (°C)	Ti 2p (at%)	Cr 2p (at%)	Fe 2p (at%)	Mn 2p (at%)	Total (at%)
700	68.6	19.6	3.0	8.3	100
600	80.5	10.5	2.6	5.9	100
550	93.1	5.0	0	1.9	100
500	96.2	3.8	0	0	100
400	100	0	0	0	100

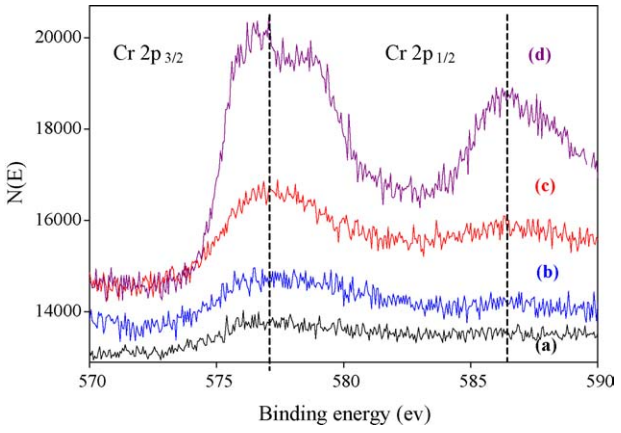

Fig. 8. High resolution XPS spectra of Cr 2p region of PPMSGF-50 films (two dip coating layers) at different calcination temperatures (a) 500 °C, (b) 550 °C, (c) 600 °C and (d) 700 °C.

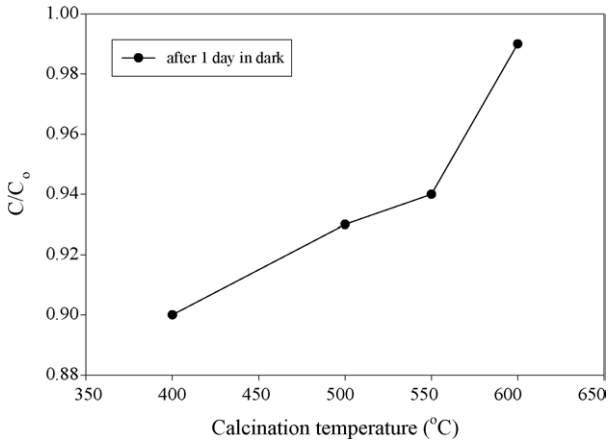

Fig. 9. Adsorption of 4-CBA in the dark, pH 2.97, 22.5 °C. PPMSGF-50 films (two dip coating layers) at different calcinations temperatures.

XPS spectra of the Cr 2p region of PPMSGF-50 films (two dip coating cycles) at different calcination temperatures were performed and the results are presented in Fig. 8. The XPS spectra show that the peak intensity increases with an increase in calcination temperature from 500 to 700 °C. The Cr $2p_{3/2}$ peak of PPMSGF-50 films prepared at calcination temperatures from 500 to 600 °C is at 576.95 eV, which demonstrates the presence of Cr_2O_3 [21,22]. It is also interesting to note that there are two Cr $2p_{3/2}$ peaks in the spectra of PPMSGF-50 films prepared at 700 °C, the binding energy of the main peak is at 576.95 eV and that of the small peak is at 578.5 eV. Considering that the binding energy of Cr 2p for CrO_3 is at 578.3 eV [23], these results suggest that the small peak in the Cr 2p region corresponds to CrO_3, which may be due to the transformation of part of Cr^{3+} into Cr^{6+} at higher oxidation temperature. Therefore, it can be concluded that the main form of chromate on the surface of PPMSGF-50 films prepared at 700 °C is Cr^{3+}, while the amount of Cr^{6+} is much smaller.

3.5. Effect on adsorption capacity

It is well known that the surface area of TiO_2 is an important factor that influences photocatalytic activity [24–27]. Adsorption studies of 4-CBA on PPMSGF-50 films immobilized on stainless steel and calcined at different temperatures were performed in order to obtain additional insights on the surface area of such films. Such adsorption studies for immobilized films can provide information of the actual effective surface area of the catalyst that can be utilized for adsorption of organic contaminants in water and may have an advantage over N_2 adsorption (BET) analysis of samples of PPMSGFs-50 films scratched from the stainless steel support. Furthermore, the adsorption capacity can be correlated with the number of effective active sites. Fig. 9 shows the relationship of normalized remaining concentration 4-CBA in water as a function of calcination temperature of PPMSGF-50 films. The results clearly show that the adsorption capacity decreases as the calcination temperature increases. In order to better explain the adsorption capacity of the PPMSGFs-50, the specific surface area of the PPMSGFs-50 was analyzed by Micromeritics TriStar 3000 Gas Absorption Analyzer. The samples were obtained by scratching the films from the stainless steel substrate after calcination. According to the result of N_2 adsorption (BET) analysis presented in Table 1, it can be seen that the specific surface area decreases as the calcination temperature increases. Therefore, the enhancement of the specific surface area is an important reason for the increased adsorption capacity caused by decreasing the calcination temperature. Based on the above discussion, it can be concluded that the total surface area and number of effective active sites of such films decrease as the calcination temperature increases.

3.6. Effect on strength of adhesion of the film

The mechanical stability of the films is a very important aspect for applications dealing with water purification. The critical loading at which the film flakes out was examined by scratch test to quantitatively compare the adhesion of PPMSGF-50 films at different calcination temperatures. Fig. 10(a) shows the result of scratch test for PPMSGF-50 film at 500 °C. The computer-logged data obtained from the scratch test include applied load, transverse force, and acoustic emission signal. Fig. 10(b) shows an optical microscope image of the scratch tracks on a PPMSGF-50 film prepared at 500 °C. The critical loading can be determined by acoustic signal generated during the scratch test combined with the observation of the optical microscope of the scratch tracks. The critical load should correspond to a burst in the acoustic signal, which indicates either debonding or cracking of the coating on the substrate. As it can be observed from Fig. 10(b), debonding or crack formation takes place as the applied loading increases. The distance from the beginning to the point where debonding or crack formation takes place is approximately 0.21 cm, which corresponds to 1.25 kg critical loading. Table 4 shows scratch test results for all PPMSGF-50 films at different calcination temperatures. It can be clearly seen that the critical loading of the film increases with an increase in calcination temperature. These results demonstrate that increasing calcination temperature results in an enhancement of film mechanical stability. In order to determine if the

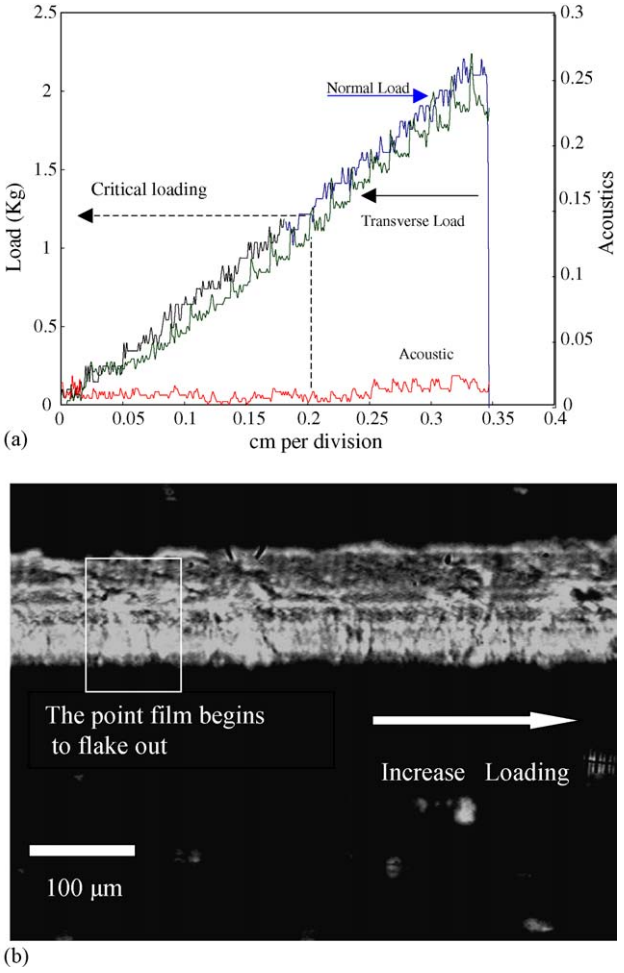

Fig. 10. (a) Scratch test of PPMSGF-50 film calcined at 500 °C and (b) optical microscope picture of the film.

adhesion of PPMSGF-50 films on stainless steel is good enough for application in water purification, these films were also tested by the cross-hatch adhesion test according to ASTM method D 3359B-02 [19] and the results are presented in Table 4. The results of the test reveal that 500 °C is a critical calcination temperature. Calcination temperatures ≥500 °C yield films with good adhesion to the stainless steel support. The mechanical stability of PPMSGF-50 films at 500 °C was also evaluated using a water circulation test under a high flow rate (1.34 L/min). During the test, no visible TiO_2 powders in water could be seen, which demonstrated that there was no significant attrition of TiO_2 particles from the film into ultra-pure water after 72 h of water circulation at such a high flow rate. Therefore, PPMSGF-50 films on stainless steel prepared at 500 °C calcination temperature showed good mechanical stability for applications in water treatment.

Table 4
Adherence of PPMSGF-50 films to the stainless steel substrate at different calcination temperatures

Temperature (°C)	400	500	550	600	700
Critical loading (kg)	0.15	1.25	1.48	1.92	–
Tape test	2B	4B	4B	4B	5B
Rank (tape test)	Fair	Good	Good	Good	Excellent

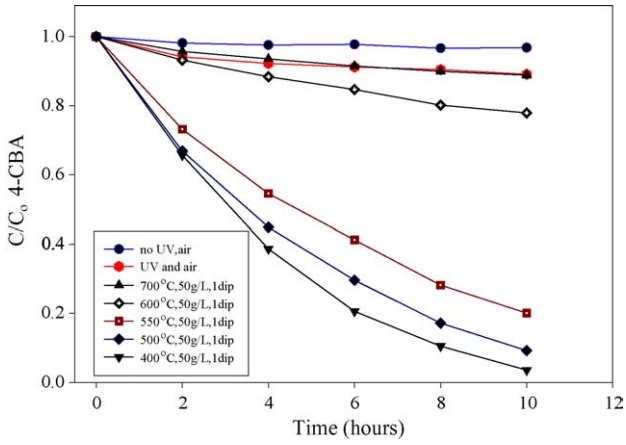

Fig. 11. Photocatalytic degradation of 4-CBA contaminant in water. Conditions: UV 300–400 nm (peak at 365 nm), air flow 2 L/min, pH 3.0 and initial concentration of 48 mg/L. Film preparation conditions: one dip coating layer.

3.7. Effect on photocatalytic activity

Fig. 11 presents results for the photocatalytic oxidation of 4-CBA in water at pH 3.0 using PPMSGF-50 films prepared at different calcination temperatures. Control tests showed that adsorption of 4-CBA in the reactor vessel was negligible and that a small amount of 4-CBA was degraded by photolysis (absence of TiO_2 films) from the lower wavelength UV radiation. The results show that there is almost no photocatalytic activity for PPMSGF-50 films prepared at 700 °C. This is most probably due to the combined effect of the decrease in surface area and the excessive concentrations of chromium and other foreign metals species in the film. In addition, transformation of most anatase into rutile may also contribute to the significant reduction in photocatalytic activity [28,29]. The photocatalytic degradation of 4-CBA for films prepared at calcination temperatures in the range between 400 and 600 °C was significantly higher. In fact, decreasing calcination temperature in the range between 700 and 400 °C leads to an increase in photocatalytic activity. This is because of the enhancement of adsorption capacity of the PPMSGF-50 caused by enhanced BET surface area (refer to Fig. 9 and Table 1). As shown in Table 1, the total pore volume of PPMSGF-50 is 0.054, 0.103 and 0.142 cm^3/g at 700, 600 and 500 °C, respectively. The higher pore volume of films calcined at 500 °C compared to those calcined at higher temperatures is attributed to the enhanced pore volume among the crystallites at lower temperature. At higher temperatures, the film porosity is reduced because of compaction and sintering effects. It should also be noted that the organic content in the sol is eliminated at temperatures ≥500 °C (refer to Fig. 4), so this is not a parameter that influences this pore volume difference. Increased pore volume is beneficial to the increase not only in film surface area but also in the number of Degussa P-25 crystallites that are exposed to solution and can serve as sites for adsorption and reaction for 4-CBA and intermediate products. In addition, the smaller crystal size of TiO_2 crystallites formed from alkoxide hydrolysis also

Table 5
Observed apparent reaction rate constant and extent of 4-CBA removal

Calcination temperature (°C)	400	500	550	600
4-CBA removal (%)	96.5	90.8	80.0	22.1
Rate constant[a] (h^{-1}/cm^2)	7.76×10^{-4}	5.84×10^{-4}	4.09×10^{-4}	6.98×10^{-5}
R^{2}[b]	0.9637	0.9874	0.9971	0.9758

[a] Based on the area for the two sides of the coated stainless steel support: total 384 cm^2.
[b] Square of linear correlation coefficient for a semi-log plot of concentration vs. time assuming pseudo first order kinetics.

contributes to an increase in the number of crystallites exposed to the solution. Therefore, it is believed that increased number of the two types of crystallites exposed to the solution is one of the reasons for the increased photocatalytic activity. As presented in Table 1, the BET of PPMSGF-50 at 400 °C is higher than that of the films prepared at 500 °C, although these films have similar pore volumes. The results shown in Fig. 4 for TGA analysis indicate that the organic content cannot be effectively eliminated at 400 °C calcination. Therefore, the remaining amount of organic content may have caused a decrease in the pore volume of the PPMSGF-50 at 400 °C calcination. Table 5 presents the observed reaction rate constants determined for PPMSGF-50 films prepared at different calcination temperatures. The observed reaction rate constant decreases with an increase in calcination temperature. In addition, according to XPS results on the surface metal composition, the concentration of foreign metals (i.e. Cr) decreases with a decrease in calcination temperature and this may be another parameter for the enhanced photocatalytic activity observed at lower calcination temperatures. It is interesting to note that the photocatalytic activity decreases significantly from 550 to 600 °C. Fig. 9 also shows that the amount of 4-CBA adsorbed on PPMSGF-50 films calcined at 550 °C is six times that of PPMSGF-50 films calcined at 600 °C. At the same time, the BET of PPMSGF-50 at 550 °C is 47.08 m^2/g, approximately 1.5 times that of PPMSGF-50 calcined at 600 °C. Therefore, a remarkable increase in BET should be an important reason for the significant increase in the number of crystallites on which the 4-CBA can be adsorbed. As a result, the photocatalytic activity was significantly enhanced at 500 and 550 °C. In addition, previous studies have shown that transition metal ions function as electron–hole recombination centers, which lead to a decrease in photocatalytic activity [17,30,31]. Therefore, a remarkable decrease in the number of Cr^{3+} on the surface of the films is most probably another important reason for the enhancement of photocatalytic activity at lower calcination temperatures. Considering that good adherence to the support is also an important aspect for the application of immobilized photocatalytic films in water purification, we believe that 500 °C is the optimum calcination temperature for preparing PPMSGF-50 films under the conditions investigated in this study.

4. Conclusions

Our results showed that calcination temperature has great effect on the surface chemical composition, mechanical stability and photocatalytic activity of TiO_2 films prepared with a combined alkoxide sol–gel and colloidal suspension preparation route. Decreasing calcination temperature in the range between 400 and 700 °C causes an increase in the photocatalytic activity of the TiO_2 films. Increased number of surface active sites caused by enhanced specific surface area and decreased foreign metal ion concentration on the surface of the films are the main reasons for such an improvement of photocatalytic activity. Increasing calcination temperature leads to an increase in adhesion strength of the coatings on the stainless steel substrate. However, the critical calcination temperature is 500 °C since the mechanical stability of films prepared at this and higher temperatures was good. The optimum calcination temperature for the synthesis of high performance PPMSGF-50 films is 500 °C since at this temperature both enhanced photocatalytic activity and good mechanical stability can be obtained. It was found that decreasing calcination temperature results in a decrease in the diffusion of foreign metal ions (i.e. Cr^{3+}) from the support to the film, which is beneficial to avoid secondary pollution, especially in applications for drinking water purification.

Acknowledgments

This work was funded in whole by a grant from the Office of Biological and Physical Research of the National Aeronautics and Space Administration (NASA) (NRA Grant number NAG 9-01475).

References

[1] A. Fujishima, K. Honda, Nature 238 (1972) 37.
[2] M.R. Hoffmann, S.T. Martin, W. Choi, D.W. Bahnemann, Chem. Rev. 95 (1995) 69.
[3] R. Molinari, M. Mungari, E. Drioli, A. Di Paola, V. Loddo, L. Palmisano, M. Schiavello, Catal. Today 55 (12) (2000) 71.
[4] M.A. Fox, M.T. Dulay, Chem. Rev. 93 (1993) 341.
[5] A. Fujishima, K. Hashimoto, T. Watanabe, TiO_2 Photocatalysis—Fundamentals and Applications, BKC, Tokyo, Japan, 1999.
[6] O. Legrini, E. Oliveros, A.M. Braun, Chem. Rev. 93 (1993) 671.
[7] A.L. Linsebigler, G.Q. Lu, J.T. Yates, Chem. Rev. 95 (1995) 735.
[8] D.F. Ollis, H. Al-Ekabi (Eds.), Photocatalytic Purification and Treatment of Water and Air, Elsevier Science Publishers BV, Amsterdam, The Netherlands, 1993.
[9] D.F. Ollis, E. Pelizzetti, N. Serpone, Environ. Sci. Technol. 25 (1991) 1522.
[10] E. Pelizzetti, C. Minero, Electrochim. Acta 38 (1993) 47.
[11] G. Balasubramanian, D.D. Dionysiou, M.T. Suidan, V. Subramanian, I. Baudin, J.-M. Laîné, J. Mater. Sci. 38 (2003) 823.
[12] G. Balasubramanian, D.D. Dionysiou, M.T. Suidan, I. Baudin, J.-M. Laîné, Appl. Catal. B: Environ. 47 (2004) 73.
[13] Y.J. Chen, D.D. Dionysiou, Podium Presentation at the 35th International Conference on Environmental System (ICES) and the 8th European

Symposium on Space Environmental Control Systems (ESSECS), July 11–14, Rome, Italy, 2005.
[14] J.G. Yu, J.C. Yu, W.K. Ho, Z.T. Jiang, New J. Chem. 26 (2002) 607.
[15] C. Guillard, B. Beaugiraud, C. Dutriez, J.-M. Herrmann, H. Jaffrezic, N. Jaffrezic-Renault, M. Lacroix, Appl. Catal. B: Environ. 39 (2002) 331.
[16] M. Keshmiri, M. Mohseni, T. Troczynski, Appl. Catal. B: Environ. 53 (2004) 209.
[17] A. Fernández, G. Lassaletta, V.M. Jiménez, A. Justo, A.R. González-Elipe, J.M. Herrmann, H. Tahiri, Y. Ait-Ichou, Appl. Catal. B: Environ. 7 (1995) 49.
[18] Y.J. Chen, D.D. Dionysiou, Appl. Catal. B: Environ., in press.
[19] American Society for Testing and Materials, ASTM, West Conshohocken, PA, D-3359-02 cross-cut tape test for adhesion.
[20] O.K. Varghese, D.W. Gong, M. Paulose, C.A. Grimes, E.C. Dickey, J. Mater. Res. 18 (2003) 156.
[21] J.F. Moulder, W.F. Stickle, P.E. Sobol, K.D. Bomben, Handbook of X-ray Photoelectron Spectroscopy, Physical Electronics Division, Perkin-Elmer Corporation, 1992.
[22] D.W. Hwang, H.G. Kim, J.S. Jang, S.W. Bae, S.M. Ji, J.S. Lee, Catal. Today 93–95 (2004) 845.
[23] G.C. Allen, M.T. Curtis, A.J. Hooper, P.M. Tucker, J. Chem. Soc., Dalton Trans. 16 (1973) 1675.
[24] L. Zhang, Y.F. Zhu, Y. He, W. Li, H.B. Sun, Appl. Catal. B: Environ. 40 (2003) 287.
[25] X.F. You, F. Chen, J.L. Zhang, J. Sol–Gel Sci. Technol. 34 (2005) 181.
[26] K. Tennakone, W.C.B. Kiridena, S. Punchihewa, J. Photochem. Photobiol. A: Chem. 68 (1992) 389.
[27] S.-C. Jung, S.-J. Kim, N. Imaishi, Y.-I. Cho, Appl. Catal. B: Environ. 55 (2005) 253.
[28] J.G. Yu, H.G. Yu, B. Cheng, X.J. Zhao, J.C. Yu, W.-K. Ho, J. Phys. Chem. B 107 (2003) 13871.
[29] Y. Tanaka, M. Suganuma, J. Sol–Gel Sci. Technol. 22 (2001) 83.
[30] H.C. Chan, J.F. Porter, J.P. Barford, C.K. Chan, J. Mater. Res. 17 (2002) 1758.
[31] J.-M. Herrmann, H. Tahiri, C. Guillard, P. Pichat, Catal. Today 54 (1999) 131.